

## EXPERIMENTAL ANALYSIS OF SOLAR AIR HEATER USING POLYGONAL RIBS IN ABSORBER PLATE INTEGRATED WITH PHASE CHANGE MATERIAL

by

**Varun Kumar BALAKRISHNAN<sup>a\*</sup>, Manikandan GURUNATHAN<sup>a</sup>,  
Rajesh Kanna PARTHASARATHY<sup>b</sup>, and Venkata Reddy POLURU<sup>c</sup>**

<sup>a</sup>Velammal College of Engineering and Technology, Madurai, India

<sup>b</sup>College of Engineering and Computing, AL Ghurair University, Dubai, UAE

<sup>c</sup>Amity University, Dubai, UAE

Original scientific paper

<https://doi.org/10.2298/TSCI210518345V>

*Heat transfer enhancement in solar air heater has been investigated by implementing rough surfaces in the absorber plate. We use paraffin wax is used as phase change material integrated with solar air heater as a thermal energy storage system. A maximum convective heat transfer is attained during the daytime and retained as latent heat to discharge heat during OFF radiation. In this investigation, two types of absorber plates were employed such as flat and polygonal-shaped ribs at the test section. Further to investigate the heat transfer enhancement, the research was conducted with and without phase change material. The study was carried out at the mass-flow rates of 0.062 kg/s, 0.028 kg/s, and 0.01 kg/s to ascertain the enhancement of thermal efficiency and heat discharge duration. The temperatures of absorber plate,  $T_p$ , ambient  $T_{amb}$ , outlet,  $T_{out}$ , and phase change material along with solar intensity,  $I$  [ $Wm^{-2}$ ], were taken as the main parameters. The research reveals that the absorber plate with polygonal ribs tested with phase change material yields a higher temperature of 77 °C with a mass-flow rate of 0.062 kg/s during peak radiation. Discharged heat energy from phase change material to absorber plate for 3.5 hours with a maximum temperature of 7.1 °C.*

Key words: solar air heater; phase change material paraffin wax,  
thermal efficiency, thermal energy storage

### Introduction

The availability of solar radiation in the southern region of India is more than nine months. In recent decades, people aware of the significance of consuming renewable energy for their daily usage such as boiling water, drying agricultural products, *etc.* through solar radiation applications like solar air heaters (SAH), solar water heaters, *etc.* were increasing commonly in rural and remote areas. However, the thermal efficiency of the existing applications was very low owing to the lack of availability of reliable solar radiation on all days, climatic conditions, and the flat shape of the absorber plate produces less relative heat transfer between the surface and working fluid. Many researchers suggest a passive technique (rough geometry) is a significant approach to increase the thermal efficiency in solar air heater. The research was elaborately validated and proved experimentally and numerically. Kumar *et al.* [1] reported a comparative review of different shapes of rib with varying pitch distance and the rib height

\* Corresponding author, e-mail: bvarunkumar09@gmail.com

in the SAH. The authors reveal implementing artificial roughness in SAH has a promising augmentation of thermal performance than a smooth surface. Moreover, researchers focus on integrating thermal energy storage (TES) in SAH, to avail heat energy during the absences of radiation [2]. Asgharian and Baniasad *i.e.* [3] presented a recent advancement in TES in SAH has a review report to show rapid charging of heat energy in phase change material (PCM) to improve thermal efficiency during peak radiation (daytime) and discharging heat energy after sunset (nighttime). The report reveals the discharging duration of heat energy, has extended for a maximum duration of 1.5 hours after sunset owing to implementing a rough plate in absorber plate integrated with PCM.

Kabeel *et al.* [4] investigated on flat and V-corrugated absorber plates in SAH, by analyzing two different thickness layers [4 cm and 2 cm] of PCM-paraffin wax individually to ascertain better enhancement of heat transfer and increasing discharge duration. The result reveals that 4 cm thickness of PCM temperature maintained between 1.5-7 °C for 3.5 hours and the temperature 1.5-5.5 °C sustained for 2.5 hours in 2 cm thickness layer at the mass-flow of 0.062 kg/s. Further, Kabeel *et al.* [5] extended investigation in finned plate SAH, with and without PCM for the same parameters. The reports proved discharge duration has increased maximum of 4 hours and temperature ranges at a maximum of 8.6 °C by consuming 39 kg of PCM and reveal thermal efficiency has increased 10.8-13.6%. Aymen *et al.* [6] experimentally studied flat plate solar air collector in a rectangular cavity, with and without PCM material to validate the thermal performance. It shows, integrating PCM, the temperature of heat discharge maintained between 3-7 °C and it observed thermal efficiency improved.

Sunil Ral and Eswarmoorthy [7] conducted an experimental investigation using V-shape of rib integrated with PCM-paraffin wax blended with Al<sub>2</sub>O<sub>3</sub> in 0.10% as latent heat storage (LHS). The 0.5 kg of capsicum, placed in SAH to remove moisture content and its results in evidence that blending nanomaterial in PCM has shown a 65% improvement in thermal efficiency. Abdullah *et al.* [8] did an experimental investigation on double pass SAH (DPSAH), with and without aluminum tin absorber plate were arranged an inline and staggered pattern. Investigated results are compared with a smooth surface plate and reveal thermal efficiency has improved 10-30% in the mass-flow rates ranges of 0.02-0.05 kg/s. Salah *et al.* [9] carried out experimental and numerical research in DPSAH in rectangular PCM-paraffin capsule. The result divulges:

- melting point delayed when increasing the mass-flow rate and
- rectangular PCM capsule precede 3 hours at 7 °C after sunset.

Moradi, *et al.* [10] conducted an experimental study in SAH using 4 cm thick layers of PCM in the mass-flow rate of 65 kg/hr.

The result exposes that maximum heat discharge temperature maintained at 4.5 °C. Abuska, *et al.* [11] studied honeycomb internal fin shape in SAH, compared with:

- flat plat,
- with PCM, and
- without PCM for identifying better thermal enhancement.

The result shows that the honeycomb model increases thermal efficiency between 2.6-23% with various mass-flow rates.

Raj *et al.* [12] investigated DPSAH with cylindrical and rectangular macro encapsulation PCM for rapid charging and discharging heat energy at a mass-flow rate of 1 kg/s. The result reveals that thermal efficiency between 47-67% has recorded with and without PCM. Srivastava *et al.* [13] conducted an experimental analysis using Lauric acid as a PCM in SAH for achieving better performances in charging heat energy. Result declared that a maximum of

50-60 °C temperature was maintained for a long duration dry the agricultural products. Azaizia *et al.* [14] did an experimental investigation in a greenhouse model, with and without PCM. The result shows 7.5 °C maintained at night time and thermal efficiency has increased by 18% from the greenhouse model. Touati *et al.* [15] conducted an experimental and numerical investigation in a simple pass air heater with PCM, later a fin plate has been engaged to validate for augmentation of thermal efficiency. The result exposes greater heat transfer has been attained. Charvat *et al.* [16] analyzed numerically and experimentally with a metal sheet and aluminum absorber plate for enhancement of thermal efficiency. It produced a good agreement owed to the thermal conductivity of the materials. Waqas and Kumar. [17] carried out a numerical analysis in PCM in winter in the mass-flow rate range of 2-8 m<sup>3</sup> per hour. The result proved it has attained higher thermal performance in the cold season. Singh and Singh [18] have been carried out the numerical analysis in single and double pass SAH with curved and flat shape absorber plates by varying pitch distance for increasing thermal efficiency. The results reveal that, by increasing the relative height and pitch distance of the geometry, thermal efficiency has possible to produce a maximum of 91.9% greater than normal.

Saxena *et al.* [19] experimentally investigated the heat transfer coefficient in cylindrical copper tube SAH integrated with granular carbon powder. The authors reveal thermal efficiency achieved a maximum of 78.1% and reached a maximum temperature of 50 °C. An experimental investigation has conducted by Ameri *et al.* [20] by implementing V-corrugator serpentine in SAH, integrating paraffin wax as a PCM in two different thermal properties (40 °C and 50 °C) at a mass-flow rate of 0.006 kg/s and 0.01 kg/s. The authors reveal, consuming higher melting temperature PCM in SAH has the maximum possible to yield greater thermal performance. Kalaiarasi *et al.* [21] investigated the thermal efficiency of flat plate solar air heater (FPSAH) using a black copper tube with synthetic therminol-55 oil as TES. The report proved that 67.7% of thermal efficiency has achieved. Experimental and numerical analysis study by Palacio [22] to prove that a greater thermal performance can attain in inclined FPSAH integrated with PCM and results compared with the normal position. The report reveals that maximum thermal efficiency has attained in the inclined SAH.

From the detailed literature survey, we have identified that rough surfaces, like the sharp and inclined shape of the ribs, yield a higher heat transfer rate than a smooth surface [23]. Besides that, PCM as a TES plays a significant performance in charging heat energy during noon and discharging heat energy after sunset. Experimentally, it is easy to design and fabricate to integrate the TES channel in SAH. Besides, various types of TES are available as organic, inorganic, and fatty materials for heating and cooling applications. The thermo-physical properties of various TES as shown in tab. 1. Among them, organics material – paraffin wax has high hydrocarbon charge heating quickly, also best melting point temperature and closer to the atmospheric temperature. Moreover, it is cheaper, more economical, yields higher thermal performance, and produces promising heat energy [4-17]. It also understands that integrating the double side inclined shape of rib with PCM in the experimental analysis has smaller quantity research and comparison of finding with flat plate study was minimum.

The primary aim of the research is to attain higher temperatures in the daytime owing to the rough plate in SAH, and integrating PCM causes the ejection of heat energy for a prolonged duration in the night time. Research initiated to implement a novel rough surface *polygonal rib* at a pitch distance of  $p = 20$  mm in the absorber plate of SAH. A significant reason behind the proposed rib shape is sharp edge and inclined angle on both sides of the rib has the maximum possible to create strong turbulence in the fluid-flow direction, causing a greater heat transfer rate. We compared the research performance with a flat absorber plate to perceive the augmen-

**Table 1. Thermo-physical property of various PCM materials**

Component	Melting temperature [°C]	Heat of fusion [kJkg <sup>-1</sup> ]	Thermal conductivity [Wm <sup>-1</sup> K <sup>-1</sup> ]	Density [kgm <sup>-3</sup> ]
Inorganics				
MgCl <sub>2</sub> -6H <sub>2</sub> O	117	168.6	0.570 (liquid, 120 °C) 0.694 (solid, 90 °C)	1450 (liquid, 120 °C) 1569 (solid, 90 °C)
CaCl <sub>2</sub> -6H <sub>2</sub> O	29	190.8	0.540 (liquid, 38.7 °C) 0.1088 (solid, 23 °C)	1562 (liquid, 120 °C) 1802 (solid, 90 °C)
Organics				
Paraffin-wax	54	173.6	0.167 (liquid, 53.5 °C) 0.346 (solid, 33.6 °C)	790 (liquid, 65 °C) 916 (solid, 24 °C)
Polyglycol E 600	22	127.2	0.189 (liquid, 38.6 °C)	1126 (liquid, 25 °C) 1232 (solid, 4 °C)
Fatty acid				
Palmitic acid	64	185.4	0.162 (liquid, 68.4 °C) –	850 (liquid, 65 °C) 989 (solid, 24 °C)
Caprylic acid	16	148.5	0.149 (liquid, 38.6 °C) –	901 (liquid, 30 °C) 981 (solid, 13 °C)

tation of thermal efficiency. Besides, paraffin wax as a PCM enforces beneath of absorber plate in SAH to extend heat discharge duration. During the investigation, a rapidly charging occurred in the PCM during peak radiation and produced higher outlet temperature. And increasing discharge duration of heat energy from PCM to absorber surface during OFF Sun.

Parameters considered for the investigation are convective heat transfer coefficient, Instantaneous thermal efficiency, and a heat transfer rate of discharging duration. It observed that they have been attained noteworthy thermal improvements in the polygonal ribbed absorber plate integrated with PCM. Also, it perceived, a rapid temperature occurred in the exit section during peak radiation and other ends noticed heat discharge extended maximum duration by integrating PCM in SAH.

#### Parameters equations

In the experimental investigation, the thermal performance of the SAH can be calculated by the following equations:

- Amount of heat energy of air [4] across the heater calculated

$$Q = \dot{m}C_p\Delta T \quad (1)$$

where  $\dot{m}$  [kgs<sup>-1</sup>] is the mass-flow rate of air inside the solar duct,  $C_p$  [Jkg<sup>-1</sup>°C] – the specific heat of the air, and  $\Delta T$  [°C] – the temperature differences of air across the heater.

- The mass-flow rate of air is calculated

$$\dot{m} = \rho_a A_c V_a \quad (2)$$

where  $\rho_a$  [kgm<sup>-3</sup>] is the density of air,  $A_c$  [m<sup>2</sup>] – the sectional collecting area, and  $V_a$  – the velocity of air at the exit of the pipe.

- The instantaneous thermal efficiency [4] of heater

$$(\eta_{\text{ther}}) = \frac{Q}{IA} \quad (3)$$

where  $I$  [Wm<sup>-2</sup>] is the total solar radiation incident on the heater.

- The convective heat transfer coefficient [24] between the air and absorber plate is given

$$h = \frac{Q}{A(T_{pm} - T_{am})} \quad (4)$$

- Daily efficiency of collectorm,  $\eta_{dp}$ , calculated

$$\eta_{dp} = \frac{\sum Q}{\sum AI} \quad (5)$$

### Experimental work

#### Experimental set-up

An experimental set-up of SAH with a rough surface has shown in figs. 1 and 2. Fabrication of investigation set-up accomplished by the guideline of ASHRAE recommendation 93-77 [25]. The major components are:

- square cavity of  $1 \times 1 \text{ m}^2$  at 10 cm height,
- the 4 mm thickness of transparent glass, positioned on the top surface of the square cavity to transmit heat radiation the absorber plate,
- the 1 mm thickness of the aluminum sheet has placed as a flat absorber plate at e mid-height (5 cm) inside the square duct,
- beneath the absorber plate-4 cm used as a PCM storage channel,
- blower and control values are used to regulate the inlet mass-flow rate, and
- the PVC pipe accustomed to connect blower and square duct.

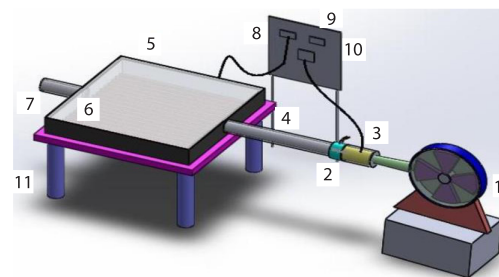


**Figure 1. Schematic diagram of solar air heater-SA**  
 SAH: 1 – blower, 2 – connecting pipe, 3 – control valve, 4 – inlet section, 5 – square duct, 6 – glass cover, 7 – outlet section, 8 – temperature sensor, 9 – manometer, 10 – solar meter, and 11 – solar collector stand



**Figure 2. Experimental set-up of SAH**

In the experimental analysis, the outcomes performance was measured and recored:

- thermocouple – to measure the temperature of the different locations in SAH as shown in fig. 4,
- a solar meter – used to measure the daily solar intensity,
- anemometer used to measure the mass-flow rate at the outlet section of the duct, and

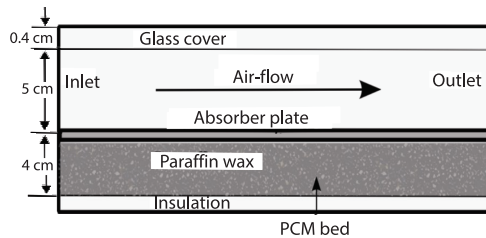


Figure 3. Sectional view of SAH

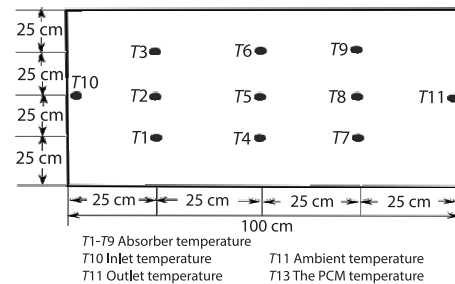
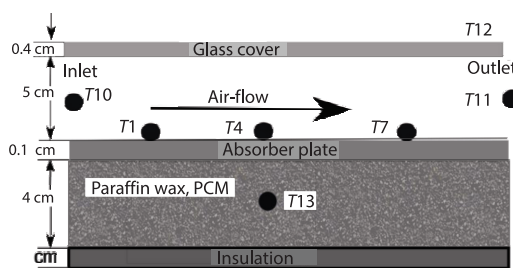


Figure 4. Position of temperature sensor in SAH; (a) sectional view and (b) top view

### Experimental procedure

An investigation was initiated to switch ON a blower for air-flows in a 5 cm gap between the glass cover and the absorber plate. The inlet velocity of air has regulated in the mass-flow rate of 0.01 kg/s, 0.028 kg/s, 0.062 kg/s. Predominantly, the experimental set-up of SAH has ensured there is no air leakage at all in the joints during the investigation. First, a flat absorber plate engaged without PCM in SAH, later replaced by a polygonal ribbed absorber plate. The calibrated digital temperature sensor has been used to record the inlet air temperature, 12 different points in the absorber plate, ambient temperature, PCM temperature, and exit temperature. The sectional view and temperatures position as shown in figs. 3 and 4.

Further, the research continues to integrate PCM in SAH – paraffin wax (as a TES) at a capacity of 38 kg stored beneath the absorber plate. The thermo-physical property of the proposed PCM – paraffin wax has shown in tab. 2. We insulated the beneath of SAH not to elude losses of

**Table 2. Thermo-physical property of the PCM – paraffin wax [4]**

Property	Values
Thermal conductivity	0.21 W/m°C
LH	190 kJ/kg°C
Melting temperature	54 °C
Solid density	876 kg/m <sup>3</sup>
Liquid density	795 kg/m <sup>3</sup>
Heat capacity	2.1 kJ/kg°C

heat energy. Research extended to repeat the aforementioned procedure for both flat and polygonal ribbed surface, with PCM in SAH and recorded the reading of temperatures. The experimental investigation has conducted in the geographical location of the Indian city, Madurai. During the month of March 19-22<sup>nd</sup> of the year 2020. The thermal performance of SAH integrated with PCM reading as compared without PCM readings to ascertain the augmentation of heat transfer. The elaborated report has discussed in the result chapter.

### The uncertainty in measurements

In experimental results, it's significant to measure the uncertainties error by the guideline of the Holman equation [26].

- manometer for measuring the flow velocity.
- The investigation was conducted using 1 mm thickness of aluminum plates as:
  - a flat absorber plate and
  - roughness absorber plate – 5 mm height of polygonal rib employed in an aluminum plate at a 20 mm pitch distance.

In that result,  $R$  is the function of independent variables ( $X_1, X_2, X_3... X_n$ ):

$$R = R(X_1, X_2, X_3, \dots, X_n) \tag{6}$$

where  $W_R$  as a result of uncertainty and  $W_1, W_2, W_3...W_n$  act as uncertainty in the independent variables  $X_1, X_2, X_3, \dots, X_n$ , respectively.

The following equation used to calculate the values of  $W_R$  [20]:

$$W_R = \left[ \left( \frac{\partial R}{\partial x_1} W_1 \right)^2 + \left( \frac{\partial R}{\partial x_2} W_2 \right)^2 + \left( \frac{\partial R}{\partial x_3} W_3 \right)^2 + \dots + \left( \frac{\partial R}{\partial x_n} W_n \right)^2 \right]^{1/2} \tag{7}$$

The relative error can be calculated:

$$E_R = \frac{W_R}{R\%} \tag{8}$$

The temperature difference across the heater, mass-flow rate of air, solar radiation intensity, thermal efficiency, useful heat gained, and the convective heat transfer coefficient of the SAH are evaluated in uncertainties and relative error equations. The values are disseminated in tab. 3.

**Table 3. Relative and uncertainties values**

Parameter	Attained values in SAH	Uncertainties	Relative error
Temperature differences [°C]	16	±0.17	0.67
Mass-flow rate [kgs <sup>-1</sup> ]	0.062 kg/s	±0.00103	1.67
Solar radiation [Wm <sup>-2</sup> ]	900	±7	0.71
Thermal efficiency [%]	77.9	±0.02	0.027
Connective heat transfer [Wm <sup>-2</sup> °C]	47.9	±0.71	1.71
Useful heat gained by SAH [W]	872.8	±8.1	1.57

### Results and discussion

The thermal performances of flat and polygonal rough surfaces in a SAH – has been examined with and without PCM to prove to attain the maximum thermal efficiency during the day-time to dry high capacity of agriculture products and prolonged heat distribution in the nighttime.

The research was initiated by a flat absorber plate in the SAH without PCM in the mass-flow rates of 0.062 kg/s, 0.028 kg/s, and 0.01 kg/s. Later, a flat plate has replaced with the polygonal ribbed absorber plate. The investigation started at 9 a. m. and protracted up to 6 p. m. Hourly heat distribution on flat absorber plate temperatures without PCM has disseminated in fig. 5 in the mass-flow rate of 0.028 kg/s. In this graph, plotted values are the average temperatures of absorber plate,  $T_p$ , ambient condition,  $T_{amb}$ , outlet temperature,  $T_{out}$ , and solar intensity,  $I$ , are recorded. It reveals, the maximum temperature of  $T_p$  reached 73 °C at peak radiation closer to noon (12.30 p. m. to 3.15 p. m. – Indian Standard Time (ISD) and later started to decrease gradually in the evening, and the ambient temperature on the day has maintained between 28-42 °C. The subsequent day, the flat absorber plate has replaced with a polygonal ribbed absorber plate and trailed the same approaches in the mass-flow rate of 0.028 kg/s. The recorded temperatures readings values plotted in fig. 6. It infers that the implementing polygonal ribbed absorber plate, the  $T_p$  temperature has adapted to raise 79 °C owing to turbulence occurred in the downstream of the flow direction in the SAH and the ambient temperature condition on the day has recorded between 29.5-43 °C. It evidences that employing rough surface *polygonal ribs* in

the absorber plate has produced a significant enhancement in thermal efficiency than the Kabeel *et al.* [4] and Aymen *et al.* [6].

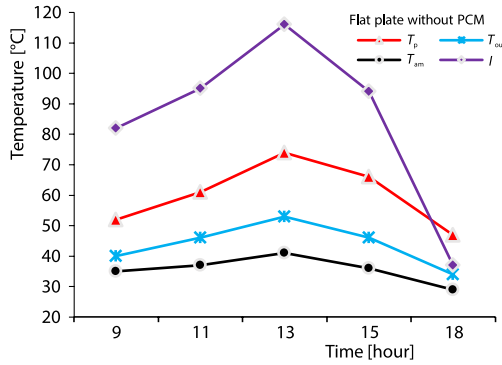


Figure 5. Temperatures of the different elements of the FPSAH without PCM, vs. time

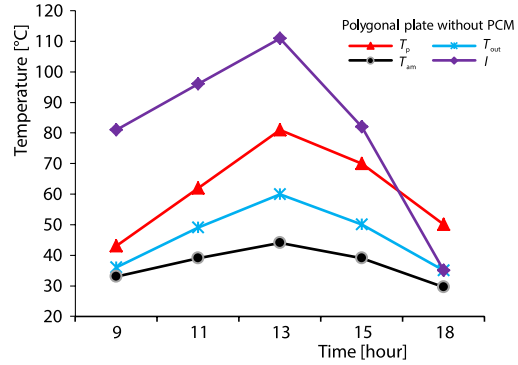


Figure 6. Temperatures of the different elements of the polygonal plate SAH without PCM, vs. time

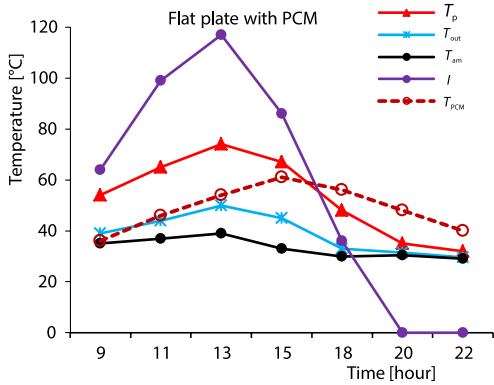


Figure 7. Hourly distribution of measured temperatures of different elements of the flat plate solar heater with PCM, vs. time

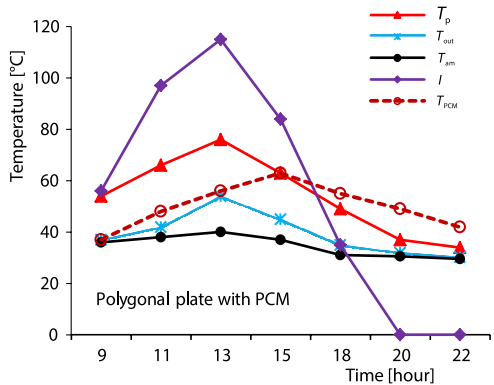


Figure 8. Hourly distribution of measured temperatures of different elements of the polygonal plate solar heater with PCM, vs. time

Further, the research extended to fill PCM-paraffin in a liquid form at 4 cm height of the PCM storage beneath of absorber plate in SAH. In this analysis, research started at 9 a. m. and protracted up to 10 p. m. to identify the maximum duration of discharging heat energy from PCM to the absorber plate. In fig. 7 shows the hourly heat distribution in a flat plate with PCM material at a mass-flow rate of 0.028 kg/s. The graph illustrates  $T_p$  has attained higher temperatures 74 °C during the peak radiation (12.30 p. m. to 3 p. m.) and maintained  $T_{amb}$  between 29 °C to 39 °C. Also, keenly observed that PCM starts melting closer to noon at a constant temperature of 54 °C and gradually charges heat energy up to 3 p. m. to maximize the outlet temperature. After sunset (6 p. m.), the distribution of heat energy from PCM to absorber plate as extended maximum to 2 hours, and the temperature of paraffin wax  $T_{PCM}$  has sustained between 1.5-4.5 °C in the mass-flow rate of 0.028 kg/s.

In the same way, a polygonal ribbed plate replaced the flat plate for investigating the possibility of improving discharge duration. Figure 8 illustrates that the highest temperature in  $T_p$  has achieved the highest temperature of 77 °C in the afternoon and maintains the ambient temperature on the day at a maximum of 40 °C. In peak radiation, higher outlet temperature occurred up to 2 p. m. owing to rapid charging, and the min-

imum deviation of temperature has maintained up to 6 p. m. After sunset PCM starts discharge heat to the surface of the absorber plate for an extreme duration of 3.5 hours with a mass-flow rate of 0.01 kg/s and sustain PCM temperature differences 2.4-7.1 °C. The study shows that the achievement of a maximum duration of heat discharge is possible by integrating PCM into the rough plate in SAH. Similarly, the discharge duration of PCM as evaluated for other mass-flow rates and revealed maximum heat discharge duration recorded in 0.01 kg/s.

In fig. 9 illustrates the comparison of temperature attained in SAH – with and without PCM in flat and polygonal ribbed absorber plate to ascertain the enhancement of thermal efficiency and the curves plotted using the formula  $[T_{out} - T_{amb}]$ . The mass-flow rate of 0.028 kg/s illustrates that polygonal ribbed without PCM outlet temperature has attained a maximum temperature difference of 16 °C and polygonal ribbed with PCM has maximum temperature of 14 °C at 1 p. m. Further, the discharge duration of heat energy from the PCM in the polygonal rib plate has a prolonged maximum duration of 3.5 hours after sunset (6.30 p. m.). It is an evidenced that implementing polygonal surfaces has produced a maximum of temperature differences than other shapes. The investigation results compared with earlier research were shown in tab. 4 to determine the maximum temperature differences attained in polygonal-shaped ribs.

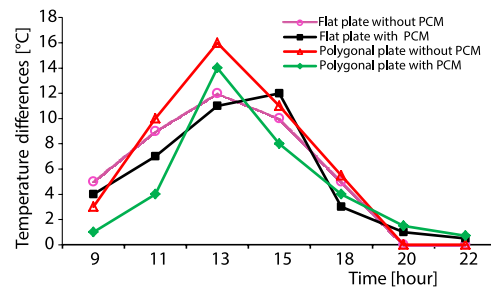


Figure 9. A comparison of the measured temperature difference of the air between polygonal and FPSAH with and without PCM when  $m = 0.028$  kg/s

Table 4. Comparison of present result with published work

Absorber plate	PCM material	Mass-flow rate [kgs <sup>-1</sup> ]	Thermal performance [%]	Temperature differences [°C]
V-corrugated serpentine [19]	Paraffin wax	0.006 and 0.01	53.1-62.6	5
Black copper tube [20]	Therminol-55	0.017, 0.02, 0.028	67.7	-
Flat plate [6]	Paraffin wax	0.018 and 0.055	34	5-7
Present study (polygonal rib)	Paraffin wax	0.062, 0.028 and 0.001	51	7.1

The thermal efficiency in SAH as evaluated by instantaneous efficiency using the eq. (3) and calculated results have plotted in figs. 10-12 in the mass-flow rate of 0.062 kg/s, 0.028 kg/s, and 0.01 kg/s, respectively. In fig. 10 illustrates that greater thermal efficiency as achieved from 10 a. m. onwards in the polygonal rib absorber plate – without PCM in the mass-flow rate of 0.062 kg/s and rapid improvement recorded in polygonal rib with PCM absorber plate from 10 a. m. to 1 p. m., later gradual decrement registered throughout a day depends on the availability of solar radiation. In fig. 8 strongly agreed that the polygonal ribbed absorber plate has attained maximum thermal efficiency than the flat plate. Owing to the strong vortex generated in the fluid-flow direction and causes higher convective heat transfer. In the same way, figs. 11 and 12 at the mass-flow rate of 0.028-0.01 kg/s infers that the maximum instantaneous efficiency as attained between 51-29% in the polygonal rib absorber plate.

However, integrating PCM in SAH, thermal efficiency increases gradually – (charging duration) up to the peak time between 11.30 a. m. to 3 p. m., later gradually sustaining the heat energy up to solar radiation, nearly 6.30 p. m. In figs. 11 and 12 illustrates, at a low mass-flow rate, the discharging duration of heat energy after sunset (6.30 p. m.) has been increasing in both

flat and polygonal rib plates. The distribution of heat energy from PCM to the absorber plate has occurred a maximum of 3.5 hours (6.30 p. m. to 10 p. m.). It shows that the achievement of thermal efficiency has 40% greater in the polygonal rib absorber plate than the flat absorber plate.

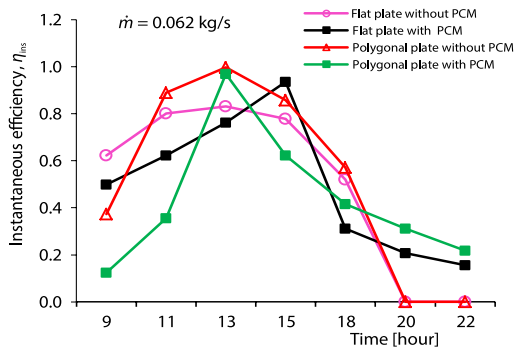


Figure 10. A comparison of instantaneous thermal efficiency between polygonal and FPSAH with and without PCM in  $\dot{m} = 0.062 \text{ kg/s}$

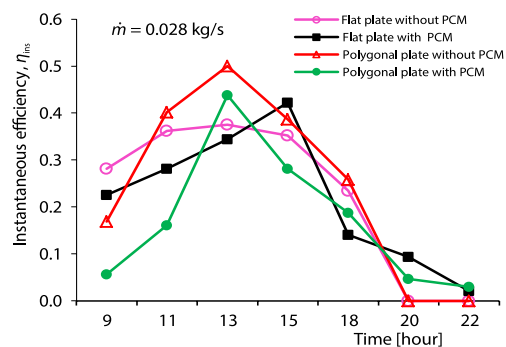


Figure 11. A comparison of instantaneous thermal efficiency between polygonal and FPSAH with and without PCM in  $\dot{m} = 0.028 \text{ kg/s}$

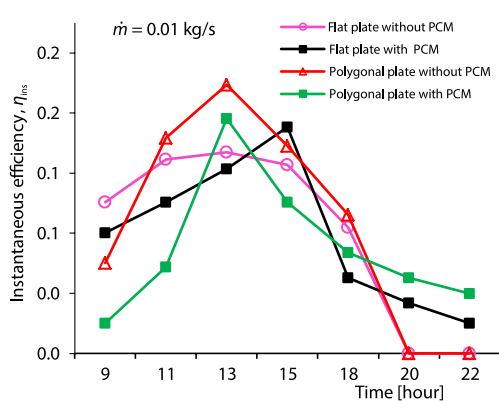


Figure 12. A comparison of instantaneous thermal efficiency between plate polygonal solar and FPSAH with and without PCM in  $\dot{m} = 0.01 \text{ kg/s}$

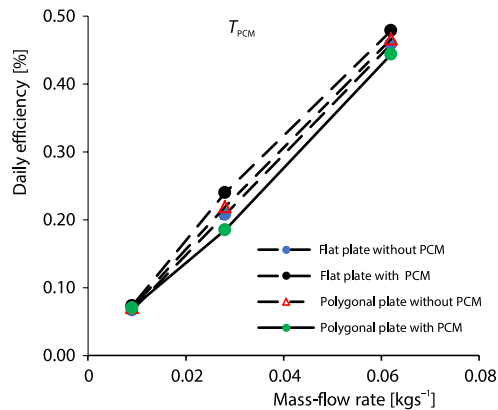
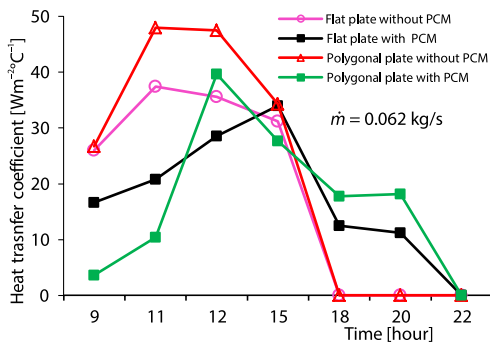
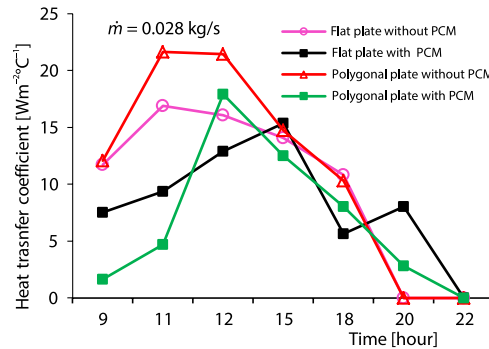


Figure 13. A comparison of daily efficiency between polygonal and FPSAH vs. the mass-flow rates with and without PCM

In this SAH experimental work, the daily efficiency is noteworthy to measure the accumulative heat gained from the collector to cumulative solar input to the heating surface. It is also imperative to compare the daily efficiency of flat absorber plates with polygonal ribbed absorber plates of SAH with and without PCM at different mass-flow rates. The recorded values as plotted in fig. 13. It illustrates that integrating PCM in flat and polygonal rib plates has a prolonged discharge duration of heat energy after sunset. We perceived that at higher mass-flow rate is produced maximum thermal efficiency at daytime – rapid charging is possible, and in the lower mass-flow rate it performed to increase heat discharge for a maximum duration in OFF radiation. It concluded that the presence of PCM – paraffin wax in the SAH was more economical and to maximize thermal efficiency. Besides, the rough surface absorber plate has too substantial for rapid charging for augmentation of heat energy than the flat plate.



**Figure 14. Convective heat transfer coefficient of air in polygonal and FPSAH via time with and without PCM when  $\dot{m} = 0.062$  kg/s**



**Figure 15. Convective heat transfer coefficient of air in polygonal and FPSAH via time with and without PCM when  $\dot{m} = 0.028$  kg/s**

A prominent part of this research work is to examine the convective heat transfer coefficient. The thermal performances of polygonal ribbed and flat absorber plate values are calculated from eq. (4), and their results are plotted in figs. 14-16 in the mass-flow rates of 0.062 kg/s, 0.028 kg/s, and 0.01 kg/s. In figs. 14-16 illustrates that the mass-flow rate of 0.062 kg/s has produced a superior heat transfer than other mass-flow rates due to its strong re-circulation flow occurring in the duct to cause higher outlet temperature. It also evidences that the polygonal rib plate with PCM has achieved a higher heat transfer rate - between 11 a. m. to 3 p. m. than the flat plate. And heat discharge duration after 6.30 p. m. was rapidly decreased to reach ambient temperature than other mass-flow rates. In fig. 15. shows similar heat augmentation fig. 14 and gradually increasing heat discharging duration than mass-flow rate 0.062 kg/s. In fig. 16 illustrates that a mass-flow rate of 0.01 kg/s has protracted the discharge duration of heat energy from PCM to the absorber surface in both the plates, and it has prolonged up to 3.5 hours in polygonal rib absorber plate then it decreasing to attained ambient temperature. It divulges that at a lower mass-flow rate, the discharging duration has increased than others.

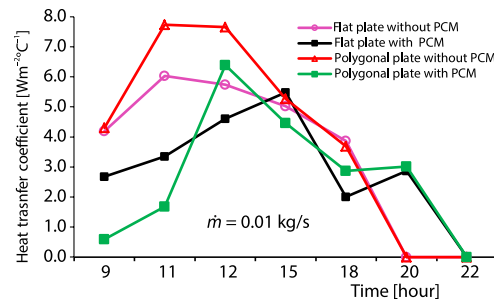


**Figure 16. Convective heat transfer coefficient of air among polygonal and FPSAH via time with and without PCM when  $\dot{m} = 0.01$  kg/s**

### Conclusions

An experimental analysis of SAH integrated with paraffin wax as a TES has been examined the thermal performances in the flat and polygonal ribbed absorber plates. The research was conducted with and without PCM in SAH to identify and compare the enhancement of thermal efficiency. It has been observed that the polygonal ribbed plate with PCM has yields higher thermal performance than the flat plate cases. From the experimental study, the significant outcomes of the research are as follows.

- The absorber plate with Polygonal ribs has produced higher convective heat transfer than the flat absorber plate due to the strong turbulence that has occurred in the flow direction.
- Paraffin wax – PCM has economical, cheaper and rapidly-produce higher thermal energy than others.

- In SAH without PCM, the outlet temperature of the polygonal rib attained 79 °C, and the flat plate reached a maximum of 73 °C.
- In SAH with PCM, the outlet temperature of the polygonal rib plate has achieved 77 °C during the peak time and after the sunset (6.30 p. m.), the temperature differences descents from 7.1-2.4 °C and a prolonged maximum of 3.5 hours. In a flat plate, temperature attained 74 °C in the daytime, and PCM temperature differences descents from 1.5-4.1 °C for 2 hours.
- The instantaneous thermal efficiency of polygonal rib without PCM has achieved higher than flat one with the mass-flow rate of 0.062 kg/s.
- A higher mass-flow rate has increased the charging duration (absorber plate to PCM) in the daytime, and the lower mass-flow rate has increased the discharging duration (PCM to absorber plate) in the night time.
- The thermal efficiency of SAH with a polygonal ribbed plate is greater than the flat absorber plate in all mass-flow rates.

### Nomenclature

$A$  – heater projected area, [m<sup>2</sup>]  
 $A_c$  – total surface area of the plate, [m<sup>2</sup>]  
 $C_p$  – specific heat of the flowing air, [kJkg<sup>-1</sup>°C<sup>-1</sup>]  
 $h$  – convective heat transfer coefficient between the air and the absorber plate  
 $I$  – total solar radiation incident on the heater, [Wm<sup>-2</sup>]  
 $\dot{m}$  – mass-flow rate of air, [kgs<sup>-1</sup>]  
 $Q_u$  – useful thermal heat energy of the air across the heater, [kJ]  
 $T$  – Time  
 $\Delta T$  – temperature difference of the air across the heater, [°C]  
 $T_{am}$  – average temperature of air inside the heater, [°C]  
 $T_{amb}$  – ambient temperature, [°C]  
 $T_g$  – glass cover temperature, [°C]  
 $T_{out}$  – outlet temperature of air from the heater, [°C]  
 $T_p$  – absorber plate temperature, [°C]  
 $T_{pm}$  – average value of the absorber plate temperatures, [°C]  
 $T_{PCM}$  – average value of the PCM temperatures, [°C]

$t$  – thickness  
 $\sum Q$  – accumulative heat gain by air  
 $\sum AI$  – cumulative solar heat input that incident on heater surface

### Greek symbols

$\Delta$  – difference  
 $\eta_{da}$  – daily average efficiency of the heater  
 $\eta_{ins}$  – instantaneous thermal efficiency of the heater

### Subscripts

am – mean  
 amb – ambient  
 av – average  
 da – daily  
 ins – instantaneous

### Acronyms

LHS – latent heat storage  
 SAH – solar air heater  
 TES – thermal energy storage

### References

- [1] Kumar, B. V., G., *et al.*, A Performance Evaluation of Solar Air Heater Using Different Shape of Ribs Mounted in Absorber Plate – A Review, *Energies*, 11 (11), 3104, pp. 2-20
- [2] Bhushan, B., Singh, R., A Review on Methodology of Artificial Roughness Used in Duct of Solar Air Heaters, *Energy*, 35 (2010), 1, pp. 202-212
- [3] Asgharian, H., Baniasadi, E., A Review on Modelling and Simulation of Solar Energy Storage Systems Based on Phase Change Materials, *Journal of Energy Storage*, 21 (2019), Feb., pp. 186-201
- [4] Kabeel, A. E., *et al.*, Experimental Investigation of Thermal Performance of Flat and V-Corrugated Plate Solar Air Heaters with and without PCM as Thermal Energy Storage, *Energy Conversion and Management*, 113 (2016), Apr., pp. 264-272
- [5] Kabeel, A. E., *et al.*, Improvement of Thermal Performance of the Finned Plate Solar Air Heater by Using Latent Heat Thermal Storage, *Applied Thermal Engineering*, 123 (2017), Aug., pp. 546-553
- [6] Aymen, E. L., *et al.*, Solar Air Heater with Phase Change Material: An Energy Analysis and a Comparative Study, *Applied Thermal Engineering*, 107 (2016), Aug., pp. 1057-1064

- [7] Sunil Raj, B. A., Eswaramoorthy, M., Experimental Study on Hybrid Natural Circulation Type Solar Air Heater with Paraffin Wax Based Thermal Storage, *Materials Today: Proceedings*, 23 (2020), 1, pp. 49-52
- [8] Abdullah, A. S., *et al.*, Performance Evaluation of a New Counter Flow Double Pass Solar Air Heater with Turbulators, *Solar Energy*, 173 (2018), Oct., pp. 398-406
- [9] Salah, M., *et al.*, Experimental and Numerical Analysis of Double-Pass Solar Air Heater Utilizing Multiple Capsules PCM, *Renewable Energy*, 143 (2019), Dec., pp. 1053-1066
- [10] Moradi, R., *et al.*, Optimization of a Solar Air Heater with Phase Change Materials: Experimental and numerical study, *Experimental Thermal and Fluid Science*, S0894-1777 (2017), 30207-8, pp. 1 -25
- [11] Abuska, M., *et al.*, A Comparative Investigation of the Effect of Honeycomb Core on the Latent Heat Storage with PCM in Solar Air Heater, *Applied Thermal Engineering*, 148 (2019), Feb., pp. 684-693
- [12] Raj, A. K., *et al.*, A Cost-Effective Method to Improve the Performance of Solar Air Heaters Using Discrete Macro-Encapsulated PCM Capsules for Drying Applications, *Applied Thermal Engineering*, 146 (2018), Jan., pp. 910-920
- [13] Srivastava, A. K., *et al.*, Evaluation of Solar Dryer/Air Heater Performance and the Accuracy of the Result, *Energy Procedia*, 57 (2014), Dec., pp. 2360-2369
- [14] Azaizia, S. K., *et al.*, Experimental Study of a New Mixed Mode Solar Greenhouse Drying System with and without Thermal Energy Storage for Pepper, *Renewable Energy*, 145 (2020), Jan., pp. 1972-1984
- [15] Touati, B., *et al.*, Flat Plate Solar Air Heater with Latent Heat Storage, *American Institute of Physics*, 1814 (2017), 1, 020016
- [16] Charvat, P., *et al.*, Solar Air Collector with the Solar Absorber Plate Containing a PCM Environmental Chamber Experiments and Computer Simulations, *Renewable Energy*, 143 (2019), Dec., pp. 731-740
- [17] Waqas, A., Kumar, S., Phase Change Material (PCM)-Based Solar Air Heating System For Residential Space Heating In Winter, *International Journal of Green Energy*, 10 (2013), 4, pp. 402-426
- [18] Singh, A. P., Singh, O. P., Performance Enhancement of a Curved Solar Air Heater Using CFD, *Solar Energy*, 174 (2018), Nov., pp. 556-569
- [19] Saxena, A., *et al.*, Design and Thermal Performance Evaluation of an Air Heater with Low-Cost Thermal Energy Storage, *Applied Thermal Engineering*, 167 (2020), Feb., 114768
- [20] Ameri, M., *et al.*, Thermal Performance of a V-Corrugated Serpentine Solar Air Heater with Integrated PCM: A Comparative Experimental Study, *Renewable Energy*, 171 (2021), June, pp. 391-400
- [21] Kalaiarasia, G., *et al.*, Experimental Analysis and Comparison of Flat Plate Solar Air Heater with and without Integrated Sensible Heat Storage, *Renewable Energy*, 150 (2020), May, pp. 255-265
- [22] Palacio, M., *et al.*, Experimental Comparative Analysis of a Flat Plate Solar Collector with and Without PCM, *Solar Energy*, 206 (2020), Aug., pp. 708-721
- [23] Varunkumar, B., *et al.*, A CFD Approach – Investigating Thermal Performances in a Solar Water Heater Using arc-Shaped Rib with Ga-Cu and Ga-CNT Nanofluids, *Proceedins*, IEASMA International Conferences, ISBN: 978-81-947901-2-9
- [24] Kays, W. M., Crawford, M. E., *Convective Heat and Mass Transfer*, 2<sup>nd</sup> ed., McGraw-Hill, New York, USA, 1980
- [25] \*\*\*, ASHRAE, 1977. ASHRAE STANDARD, Methods of Testing to Determine the Thermal Performance of Solar Collectors, ASHRAE 1977, New York, USA, 1977, Vol. 345
- [26] Holman, J. P., *Experimental Methods for Engineers*, Tata McGraw-Hill Publishing Company Limited, New Delhi, India, 2004